生細胞における可視化プローブ

梅　澤　喜　夫*

Shining the Chemical Processes in Living Cells

Yoshio UMEZAWA

This is the first year of the Toyota fellow report. In this review, 1) nuclear receptor and coactivator/corepressor interactions, 2) imaging dynamics of endogeneous mitochondrial RNA, and 3) signal sequence in mitochondrial intermembrane space are reported. The other signaling pathways in the cells, e.g. second messengers, phosphatydyl inosytol-3,4,5-trisphosphate will be reported the year to come. STM molecular tips will be reported in the third year.

The intracellular signaling can be monitored in vivo in living cells by genetically encoded intracellular fluorescent probes. In this review, three examples of such probes were introduced; 1) nuclear receptor and coactivator/corepressor interactions, 2) imaging dynamics of endogeneous mitochondrial RNA, and 3) signal sequence in mitochondrial intermembrane space. These probes are of general use not only for fundamental biological studies, but also for assay and screening of possible pharmaceutical or toxic chemicals that facilitate or inhibit cellular signaling pathways.

INTRODUCTION

The intracellular signaling can be monitored in vivo in living cells by genetically encoded intracellular fluorescent and/or bioluminescent probes, which include second messengers, protein phosphorylation, protein-protein interactions, and protein localizations. These probes are of general use not only for fundamental biological studies, but also for assay and screening of possible pharmaceutical or toxic chemicals that facilitate or inhibit cellular signaling pathways. This article is not an encompassing review but rather presents highlights of the authors' research on three illustrative examples that were originally reported from the author's laboratory. First, our fluorescent probes are capable of distinguishing among agonists, antagonists, and selective nuclear receptor modulator (SNRMs), and can therefore serve as versatile molecular sensors that predict the pharmacological character of ligands, which is important for an accurate cure of a disease. Second, a genetically encoded fluorescent RNA probes for charactering location and dynamics of mitochondrial RNA (mtRNA) in single living cells. The probes consist of two RNA-binding domains of PUMILIO1, each connected with split fragments of a fluorescent protein capable of reconstituting upon binding to a target RNA. We designed the probes to specifically recognize a 16-base sequence of mtRNA encoding NADH dehydrogenase subunit 6 (ND6) and to be targeted into the mitochondrial matrix, which allowed real-time imaging of ND6 mtRNA localization in living cells. Finally, to identify the IMS (mitochondrial intermembrane space)-targeting sequence, we developed a simple genetic screening method to discriminate the proteins localized in the IMS from those in the mitochondrial matrix, thereby revealing the minimum requisite sequence for the IMS targeting.

2009年1月27日 受理
*豊田理化学研究所フェロー

1. NUCLEAR RECEPTOR AND COACTIVATOR/COREPRESSOR INTERACTIONS

Nuclear receptors (NRs) are transcription factors that are essential for embryonic development, the

maintenance of differentiated cellular phenotypes, metabolism, and apoptosis[1]. NRs are well-established therapeutic targets for the treatment of several diseases including diabetes and cancers, and drug development is focused on the ligands that either promote or block the NRs activities. A pure antagonist, when used as a drug, blocks the activity of its receptor in the target tissue as well as in other tissues of the body, which might cause side effects; for example, a pure estrogen receptor (ER) antagonist, ICI 182,780, effectively blocks the ER activities in the breast tissue to treat breast cancer, but at the same time it can cause osteoporosis by inhibiting the estrogen actions in bones[2]. By contrast, a selective nuclear receptor modulator (SNRM) is able to block the receptor activity by acting as an antagonist in a target tissue, but promotes the activity of the same receptor in other tissues of the body by acting as an agonist. Therefore, SNRMs that have mixed agonistic/antagonistic activities depending on the cell type, are beneficial pharmaceuticals for NR-related diseases[3)4)]. There is mounting evidence that explains how SNRMs exhibit their tissue-specific effects [3)~6)]. Ligand binding to the NR induces a conformational change in the NR LBD that allows the ligand-bound NR to interact with coregulator proteins[7)~9)]. Coactivator binding to the NR results in the activation of gene expression that is related to the NR functions, however, co-repressor binding to the NR suppresses the gene expression in the cell. Pure agonists recruit coactivators to NRs, while pure antagonists inhibit the recruitment of coactivators to NRs or recruit corepressor proteins to NRs[8)10)11)]. However, in the case of SNRMs, the ligands can recruit both coactivators and co-repressors to NRs[3)4)]. In addition, the expression levels of coactivator and corepressor proteins are known to be very different between tissues[5)]. The dose of SNRMs thus results in the tissue-specific recruitment of coactivators or corepressors to NRs. This explains the tissue-specific curing effect by SNRMs, but not by pure agonists and antagonists. The molecular basis of the SNRM function provides us with an idea for a rational method for high-throughput screening of SNRMs. Here, we describe indicators for the screening of SNRMs by using the NR LBD and the peptide sequence from NR-interacting coactivator or corepressor protein that is expressed in the target tissue. The principle of the indicators is shown in Figure 1. The progesterone receptor LBD (PR LBD)[12)] a member of NR superfamily, is attached with a coregulator peptide, either a coactivator or a corepressor[9)13)], via a flexible linker sequence. The resultant protein was inserted between cyan and yellow fluorescent proteins (CFP for the donor, and YFP for the acceptor fluorophore) in such a way that the excitation and emission spectra of CFP and YFP are suitable for fluorescence resonance energy transfer (FRET) from CFP to YFP. This fusion protein (*conpro*) functions as a fluorescent indicator in an intramolecular FRET fashion, to visualize the ligand-induced *con*formational changes in the *pro*gesterone receptor that are necessary for the NR to interact with the coactivator peptide in live cells[14)~17)]. Another indicator in which a corepressor peptide is used in place of a coactivator peptide was called *conpro* 1. The addition of an agonist to cultured cells expressed with *conpro* promotes the interaction between the PR LBD and coactivator within *conpro;* this results in an increase in the FRET from the CFP to the YFP. By contrast, an antagonist inhibits the PR LBD-coactivator interaction within *conpro*. The addition of an SNRM ligand that has mixed agonist/antagonist character promotes the PR LBD interaction with the coactivator, as well as the interaction between the corepressor within *conpro* and *conpro* 1, respectively, to increase the FRET response. This strategy was used to discriminate among NR agonists, antagonists and SNRMs. Knowledge about the conformational change(s) that are induced by a ligand in the NR LBD, which in turn enables the interaction with coregulator proteins is crucial for the understanding of the physiological action of the ligand, and would be useful for the development of NR ligands to use as therapeutic agents for an accurate cure of diseases.

In contrast to previous assay methods such as receptor binding assays, which cannot discriminate among agonists, antagonists and SNRMs, and reporter gene assays, which take over 24 h to perform, the present indicators can classify ligands into agonists, antagonists, and SNRMs within a few minutes in intact living cells, without the need for a laborious protein purification step. The present

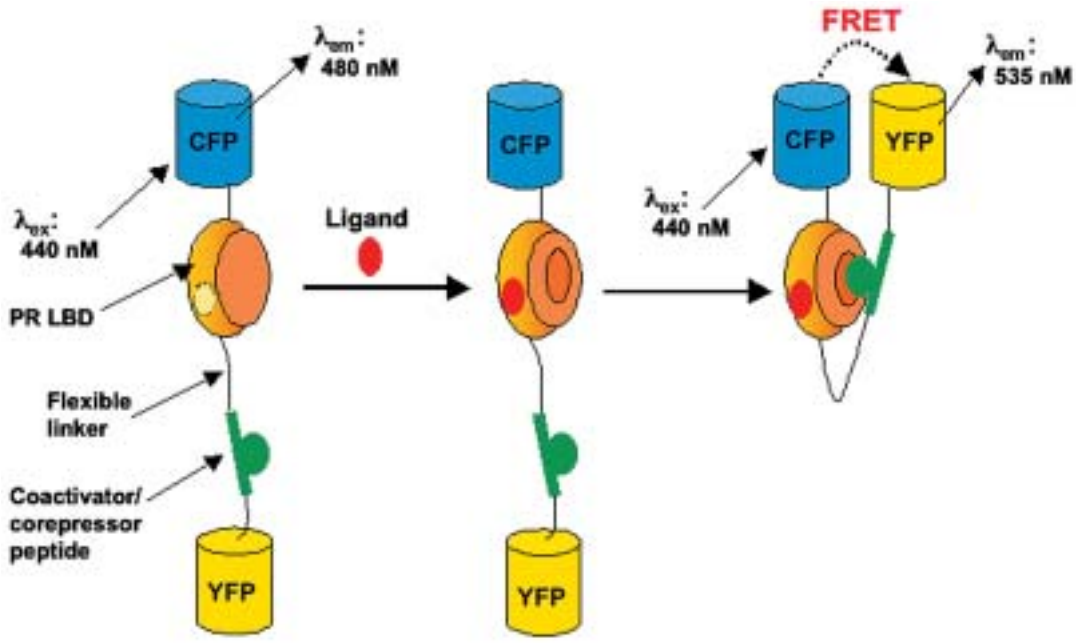

Figure 1. Fluorescent indicator for the ligand-induced coactivator/corepressor recruitment to the PR LBD in living cells A) Principle of the conpro, based on intramolecular FRET, to visualize the ligand-dependent interaction between the PR LBD and the steroid receptor coactivator 1 peptide (SRC-1)/silencing mediator for retinoid and thyroid hormone receptor (SMRT). Upon ligand binding, the PR LBD and coactivator/corepressor interact with each other. Consequently, YFP is oriented in close proximity to CFP; this results in an increase in the FRET response. The magnitude ofthe FRET increase strongly depends on the relative orientation and distance between the donor (CFP) and acceptor (YFP) fluorophore[17].

assay, which is carried out in the physiological environment of living cells, provides an insight into the importance of ligand-induced conformational change(s) to the recruitment of coregulatory proteins whose cellular concentrations influence the stimulatory or inhibitory behavior of a SNRM, and in turn, the regulation of the transactivation of a NR. The conpro assay is not intended as a read-out of the binding affinity of a drug, but rather it probes the drug's efficacy as an agonist, antagonist, or SNRM in living cells. The permeability of a drug into cells and the conformational changes that are induced in a receptor to regulate the interaction between the receptor and coactivator and/or corepressor proteins all determine the efficacy of a drug much more than a simple binding assay. The LBD of all NRs have a common overall three-dimensional structure. Therefore, the present strategy can be applied to all NRs, including orphan receptors, and it could play an important role in preclinical drug development for the treatment of several diseases.

2. IMAGING DYNAMICS OF ENDOGENEOUS MITOCHONDRIAL RNA

Localization of mRNA has an essential role in the regulation of protein expression at particular sites in living cells[18]. This function is controlled temporally and spatially by stability of the mRNA, gene expression and directed mRNA transport. In a single human cell, mitochondria contain 10^3–10^4 copies of the mtDNA, which encodes two ribosomal RNAs (rRNAs), 22 transfer RNAs (tRNAs) and 13 genes encoding polypeptides that form parts of the respiratory chain located in the inner mitochondrial membrane[19]. A noncoding regulatory region includes an origin of replication and two promoters. Transcription from these promoters generates L and H strands, which are polycistronic transcripts that are processed to produce mature rRNAs, tRNAs and mRNAs. Protein-coding regions of the resulting RNAs are translated into proteins by ribosomes in the mitochondrion. The mechanism of mitochondrial gene expression has been well studied by biochemical analysis with large populations of cells, but little is known about the dy-

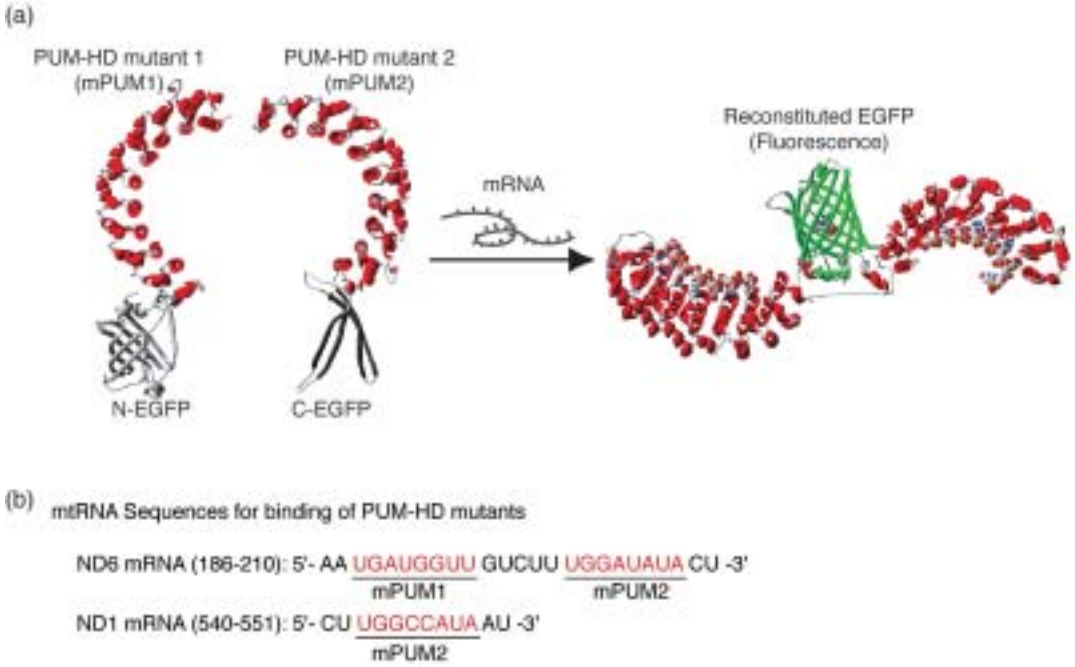

Figure 2. Detection of a target mRNA based on complementation of split EGFP fragments. (a) Schematic of the basic strategy for detecting target mRNAs. Two RNA-binding domains of PUM-HD are engineered to recognize specific sequences on a target mRNA (mPUM 1-RNA and mPUM 2-RNA). In the presence of the target mRNA, mPUM 1 and mPUM2 bind to their target sequences bringing together the N- and C-terminal fragments of EGFP, resulting in functional reconstitution of the fluorescent protein. (b) Sequences of mtRNAs that are recognized by PUM-HD mutants[25].

namics of the mtRNAs in single living cells. Methods for real-time visualization of mRNA offer essential information on RNA synthesis, processing, transport and protein expression in response to external stimuli. mRNAs labeled with molecular beacons have been used to map localization of target mRNAs[20]. The beacon is a way to specifically recognize a target RNA via Watson-Crick base paring. Potential drawbacks of using this method are that injection of beacons into living cells can damage the cells, and it is difficult to target the beacons to a distinct intracellular organelle. GFP tagging to mRNA-binding proteins is another approach to visualizing dynamics of mRNAs that function in the nucleus[21], upon generation of cellular polarity[22], asymmetric segregation in oogenesis[23] and cell migration[24]. A drawback of this approach is that it is difficult to distinguish the GFP-tagged protein bound to mRNA from the one unbound to mRNA. Additionally, the approach requires identification of a particular protein that binds uniquely to the specific mRNA of interest. To analyze the dynamics of mtRNAs, we developed genetically encoded fluorescent probes, the recognition sequences of which can be tailor-made based on a 16-base sequence of target mtRNAs. We targeted these probes into the mitochondria by connecting them to a peptide sequence of mitochondrial targeting signals. Using the probes, we visualized mtRNA of NADH dehydrogenase 6 (ND6) in single living cells. We revealed that under normal conditions the mtRNA is localized, but oxidative stress causes the mtRNA to disperse in mitochondria[25].

The basis for the RNA probe is reconstitution of split fragments of enhanced GFP (EGFP)[26][27]. Each of the fragments is fused to a sequence-specific RNA-binding domain, Pumilio homology domain 3 (PUM-HD) of human PUMILIO1 (Fig. 2a, 2b). PUM-HD is composed of an array of eight elements (repeats 1–8) that recognize the RNA sequence UGUANAUA, and each element specifically recognizes a single base[28]. Notably, specificity of PUM-HD for the RNA-base sequences can be altered by changing RNA-recognizing amino acid residues within the PUM-HD elements. Two different PUM-HDs, recognizing

two different 8-base sequences aligned in tandems, theoretically can distinguish 4^{16} (about 4.3×10^9) transcripts. Two different PUM-HDs are therefore sufficient to uniquely identify a target RNA transcribed in a single cell. In our system, upon interacting with RNA, the PUM-HDs bring the split fragments of EGFP to which they are fused close enough for the fragments to associate, reconstitute the native EGFP structure and recover fluorescence. Monitoring the fluorescence signals allows spatial and temporal analysis of mRNA localization in single living cells.

In principle, this method described here allows the visualization of any endogenous mRNAs by mutating the elements of PUM-HD according to the previously established RNA-recognition rules[28]. This has particular advantages over previous mRNA-detection methods, in which a target mRNA must be connected to a short RNA sequence that is recognized by a specific binding protein such as MS-2. The expression levels of such engineered RNAs may be different from those of the corresponding endogenous mRNA. Also, the localization of excess amounts of engineered mRNAs may be different from that of endogenous mRNA owing to a cytosolic distribution of the excess mRNA. To probe endogenous mRNAs, molecular beacons have been used to specifically recognize a target mRNA. Potential drawbacks of using molecular beacons are that it is impossible to deliver molecular beacons efficiently inside living cells or to target an intracellular organelle because beacons are generally large charged molecules.

Our estimated binding affinities of mPUM1 and mPUM2 for their cognate sequences were ～100-fold lower than the binding affinities of mutated PUMs for their cognate sequences reported earlier[28]. The discrepancy may be due to the fact that mPUM1 and mPUM2 each exhibited gradual aggregation upon preparation of the purified protein. This likely resulted in a lowering of the RNA-binding abilities of the mPUM1 and mPUM2. Despite this technical problem, we confirmed the selective binding of mPUM1 and mPUM2 to their cognate RNA sequences using these in vitro experiments. A difficulty in the analysis of the mRNA dynamics using the present method is that reconstituted EGFP or Venus remains fluorescent even after degradation of its target mRNA. This is because the dissociation rate of the fluorescent protein fragments is quite slow[29]. When the lifetime of mRNA is much longer than the chromophore maturation of EGFP or Venus, however, newly generated EGFP or Venus after photobleaching can indicate the precise localization of the target mRNA as demonstrated in the present study. Here we showed that the mtRNA is constrained within the mitochondrial matrix under normal physiological conditions, whereas oxidative stress results in the diffusion of MT-ND6 mtRNA. To date, it is poorly understood how oxidative stress leads to mtDNA instability, how mtRNA is degraded and what kinds of molecules are involved in the process. The temporal and spatial relationship between mtDNA and MT-ND6 mtRNA localization in the present study showed that MT-ND6 mtRNA is constrained on the mtDNA or in folded structures of mitochondrial matrix, and that the mtRNA dispersed after stimulation of the cells with H_2O_2. We found that degradation of mtDNA, 12S rRNA and 16S rRNA is an early event that is followed by diffusion of MTND6 mtRNA. The MT-ND6 mtRNA thus dispersed becomes unstable and gradually degrades, which may involve either a ribonuclease or the direct decomposition by reactive oxygen species. It is known that a nucleoid protein called aconitase (Aco1p) is essential for mtDNA stabilization and its maintenance, and is degraded by Lon protease after oxidative modification[30][31]. The faster degradation of mtDNA observed in this study may be caused by the decomposition of nucleoids. In contrast, 12S rRNA and 16S rRNA function cooperatively with the translational machinery of mitochondrial proteins. Therefore a plausible mechanism for mtRNA stability may be that in the physiological condition, MT-ND6 mtRNA is stabilized by the proteins associated with nucleoids or the translational machinery, which protect the mtRNA against oxidative stress. Degradation of MT-ND6 mtRNA upon H_2O_2 stimulation may be due to decomposition of the nucleoids and translational machinery proteins, resulting in destabilization of the naked mtRNA.

It is known that the ND6 protein is a part of complex I of the respiratory chain, which is essential for electron transfer in the mitochondrial inner

membrane. Malfunction of the respiratory chain causes fragmentation of tubular mitochondria[32] and a decrease in growth rates[33)34)]. Our observations demonstrate that the probes did not affect the mitochondrial morphology or motility. Additionally, the cells containing the RNA probes were alive for more than 7d without a change in apparent growth rates. These results strongly suggest that the RNA probes have little effect on the specific functions of MT-ND6 mRNA under physiological conditions.

We showed that ND6 mtRNA is localized within mitochondria and concentrated particularly on mitochondrial DNA (mtDNA). Movement of the ND 6 mtRNA is restricted but oxidative stress induces the mtRNA to disperse in the mitochondria and gradually decompose. These probes provide a means to study spatial and temporal mRNA dynamics in intracellular compartments in living mammalian cells.

3. THE SIGNAL SEQUENCE IN MITOCHONDRIAL INTERMEMBRANE SPACE

Protein-based fluorescent and functional probes are widely used for real-time visualization, purification, and regulation of a variety of biological molecules. The protein-based probes can generally be targeted into subcellular compartments of eukaryotic cells by a particular short peptide sequence. Little is known, however, about the sequence that targets probes into the mitochondrial intermembrane space (IMS). To identify the IMS-targeting sequence, we developed a simple genetic screening method to discriminate the proteins localized in the IMS from those in the mitochondrial matrix, thereby revealing the minimum requisite sequence for the IMS targeting. An IMS-localized protein, Smac/DIABLO, was randomly mutated, and the mitochondrial localization of each mutant was analyzed. We found that the four residues of Ala-Val-Pro-Ile are required for IMS localization, and a sequence of these four residues fused with matrix-targeting signals is sufficient for targeting the Smac/DIABLO into the IMS. The sequence was shown to readily direct three dissimilar proteins of interest to the IMS, which will open avenues to elucidating the functions of the IMS in live cells. Mammalian mitochondria have pivotal roles in the production of most of the cellular ATP, generation of reactive oxygen species, calcium metabolism, and cell death. Such mitochondrial functions are closely related to the proteins in the structurally complex organelle. Most mitochondrial proteins are encoded by the nuclear genome and synthesized on cytosolic ribosomes. The proteins are then targeted into the mitochondria, where the proteins are sorted to one of the submitochondrial compartments, the outer and inner membranes and two aqueous compartments, the intermembrane space (IMS), and the matrix[35)~37)]. The targeting and sorting into the mitochondrial matrix are achieved by N-terminal presequences of precursor proteins. The presequences are composed of 20–80 residues capable of folding into a positively charged amphipathic helix. The helix is recognized by specific receptors in the mitochondrial outer membrane and is then inserted into the inner membrane *via* the membrane potential. The energy generated from ATP hydrolysis by motor proteins in the matrix mediates completion of the translocation[35)]. In contrast, no uniform pathway exists into the mitochondrial IMS[35)~42)]: although several different pathways have been proposed regarding the protein transport into the IMS, no signal sequence has been identified that allows exogenous proteins to locate in the IMS. In the past decade, genetically encoded probes have often been used as powerful tools to image morphologies or ionic properties of intracellular organelles in living cells[43)]. In particular, custom-made fluorescent probes targeted into the organelles enabled real-time and quantitative analyses of the pH[44)~46)], calcium ion[47)], and redox potential[48)]. The targeting of the probes into particular organelles is generally achieved by the addition of a short signal peptide sequence to the probes of interest. Because of the ability of the signal sequences to deliver the probes exclusively into specific subcellular locations, they have also been used for intracellular antibodies (so-called intrabodies) as probes to regulate the function of target proteins in a specific organelle[49)~52)]. The targeting of the probes was accomplished in such organelles as the nucleus, endoplasmic reticulum (ER), peroxisome, and mitochondrial matrix, but little was known about the IMS-targeting sequences. To elucidate crucial roles for cellular functions of the

IMS, such as energy production, protein transport, and apoptosis, it is very important to identify the signal sequences that deliver a particular protein into the mitochondrial IMS. A mammalian protein called Smac/DIABLO is an IMS localized protein that is conserved in mammals[53)54)]. The Smac/DIABLO protein derived from *Mus musculus* is synthesized as a precursor molecule of 237 amino acids; the N-terminal 53 residues serve as the mitochondrial targeting sequence, which is removed by the inner membrane peptidase (IMP) complex after import[55)]. Thus, the mature Smac/DIABLO protein has 184 amino acids, and the four residues of the N-terminus are Ala-Val-Pro-Ile. These four N-terminal residues play an indispensable role in Smac/DIABLO function; they promote apoptosis by eliminating the inhibitory effect of the inhibitor of apoptosis protein (IAP) through physical interaction[56)~58)]. A point mutation in the four residues leads to a loss of interaction with IAP and a concomitant loss of the Smac/DIABLO function. The structural and functional aspects of Smac/DIABLO have been extensively investigated, but how the protein targets into the mitochondrial IMS remains unknown. To identify the amino acids or domains of Smac/DIABLO important for targeting into the IMS, we have developed a high-throughput screening system that enables discrimination between the proteins in the IMS and those in the mitochondrial matrix or cytosol. Using this system, we identified from Smac/DIABLO mutant libraries the amino acids necessary for the localization of the IMS. We further showed that amino acid residues 54–57 (Ala-Val-Pro-Ile), which are crucial for the apoptotic function, are also important for the IMS localization. We found that N-terminal amino acid residues 10–57 (RSVCSLFRYRQRFPVLANSKKRCFSELIKPWHKTVLTGFGMTLCAVPI) are the minimal sequence that functions as the IMS targeting signal. We demonstrated that this IMS-targeting signal is able to deliver different probe proteins and intrabodies into the IMS[59)].

Because the diameter of the mitochondria is $< 1\ \mu$m, it is impossible to discriminate the proteins localized in the mitochondrial matrix from those in the IMS by immunostaining under the optical microscope. To date, discrimination of the protein sublocalization has therefore been determined by immunogold electron microscopy or mitochondrial subfractionation followed by immunoblot analysis[60)61)]. Although these techniques are reliable and accurate, the sample preparation for electron microscopy requires many laborious steps, such as fixing the cells with resin, slicing them into thin sections, and blotting them with antibodies. Subfractionation techniques take a considerable amount of time because of the laborious electrophoresis, which limits screening and identification of the IMS-localized proteins. To bypass these steps, we developed a simple method to discriminate between the proteins localized in the mitochondrial IMS and those in the matrix or cytosol. The concept is based on reconstitution of split-enhanced GFP (split-EGFP) by protein splicing with a DnaE intein (Fig. 3)[62)]. Protein splicing is a reaction in which an intein is excised from a polypeptide precursor and then the flanking polypeptides are linked by a native peptide bond[63)]. We previously developed a new split-EGFP reporter for identifying the mitochondrial-matrix-localized proteins (Fig. 3, left)[62)]. The fluorescence of the split-EGFP reporter can be recovered by protein splicing when a protein transports into the mitochondrial matrix.

We investigated whether the N-terminal 57 residues, including Ala-Val-Pro-Ile, in Smac/DIABLO are generally able to lead a particular protein into the IMS. To demonstrate this, we engineered the cDNA that encoded a pH indicator, a yellow-emission variant of GFP (YFP(H148G)), to contain the signal sequence of the IMS and expressed it in cultured mammalian cells. We generated NIH 3T3 cells expressing the signal-sequence-connected YFP (H148G) by infecting the cells with retroviruses at an infection efficiency of 30%. A microscopic analysis revealed that YFP(H148G) was exclusively localized in mitochondria. Next, we investigated localization of YFP(H148G) in the submitochondrial compartments. Isolation of mitochondria from NIH3T3 cells showed that YFP(H148G) connected with the 57 amino acid residues remained resistant to protease digestion with trypsin. However, the YFP (H148G) was mostly degraded when the outer membrane was permeabilized with digitonin, a strong indication that YFP(H148G) is predominantly localized in the IMS. In contrast, the YFP(H148G) targeted into the mitochondrial matrix is not degraded,

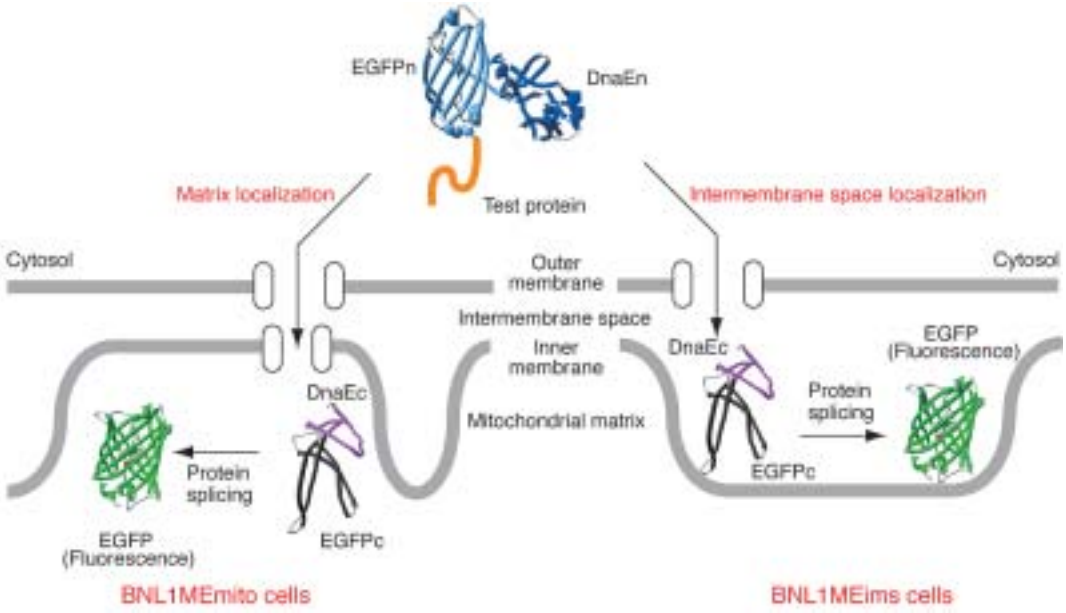

Figure 3. EGFP reconstitution by protein splicing in submitochondrial compartments. When a test protein is localized in the mitochondrial matrix (left) or in the IMS (right), N- and C-terminal DnaE are brought close together, and EGFP is formed by protein splicing in the respective compartments. BNL1 MEmito cells permanently express a fusion composed of C-terminal fragments of DnaE and EGFP in the mitochondrial matrix (left), and BNL1 MEims cells express the same fusion in the IMS (right). The blue and magenta 3D structures represent DnaEn and DnaEc, and the light blue and dark gray structures represent N- and C-terminal fragments of EGFP, respectively. The orange strand represents a test protein[59].

a sign that the inner membrane remained intact. To examine whether the YFP(H148G) is anchored in the mitochondrial inner membrane or moves freely in the IMS, we ruptured the mitochondrial outer membrane by inducing apoptosis. When YFP (H148G) was connected with the IMS signal sequence or full-length Smac/DIABLO, stimulation of the HeLa cells (derived from human carcinoma of cervix) or MCF-7 cells (derived from human breast cancer) with staurosporine (STS) resulted in the release of the YFP(H148G) from the IMS into the cytosol. In the case of YFP(H148G) targeted into the matrix, no change in the localization of YFP (H148G) was observed. These results demonstrate that the signal sequence of the mitochondrial IMS has the ability to accurately lead the exogenous indicator into the mitochondrial IMS and to allow the indicator to diffuse freely inside the organelle. To determine the pH in the IMS, we measured the fluorescence intensity of YFP(H148G) with differing pH. he cells expressing YFP(H148G) were incubated with ionophores of nigericin and monensin and then equilibrated in buffers of differing pH. FACS analysis showed an almost linear increase in fluorescence over the pH range from 7.0 to 8.5. Using this calibration, we extrapolated the pH value of the IMS targeted with the YFP (H148G) from the fluorescence intensity of the cells without the ionophore. The pH was estimated at 7.5 when the cells were in a resting state[59].

Our discovery of the signal sequence will be of great help in resolving the unknown functions of the mitochondrial IMS. We showed that the sequence readily directs any proteins into the IMS without disrupting physiological environments in the IMS. The physiological processes in the IMS are poorly understood, because no method has been known for targeting probes into the IMS. In addition, intracellular expression of engineered antibody fragments, as designed for high-affinity binding reagents, has the potential to inactivate target proteins by modifying or blocking the proteins involved in essential cellular signaling pathways. Therefore, the signal sequence of the IMS that we identified will become a powerful tool for targeting various probe molecules and intrabodies into the IMS.

REFERENCES

1) Gronemeyer H, Gustafsson J, Laudet V, Nat Rev Drug Discov **3** (2004) 950–964.
2) Ciana P, Luccio GD, Belcredito S, Pollio G, Vegeto E, Tatangelo L, Tiveron C, Maggi A, Mol Endocrinol **15** (2001) 1104–1113.
3) Liu Z, Auboeuf D, Wong J, Chen JD, Tsai SY, Tsai MJ, O'Malley BW, Proc Natl Acad Sci USA **99** (2002) 7940–7944.
4) Shang Y, Brown M, Science **295** (2002) 2465–2468.
5) Smith CL, O'Malley BW, Endocr Rev **25** (2004) 45–71.
6) Greschik H, Moras D, Curr Top Med Chem **3** 2003) 1573–1599.
7) Shiau AK, Barstad D, Loria PM, Cheng L, Kushner PJ, Agard DA, Greene GL, Cell **95** (1998) 927–937.
8) Nolte RT, Wisely GB, Westin S, Cobb JE, Lambert MH, Kurokawa S, Rosenfeld MG, Wilson TM, Glass CK, Milburn MV, Nature **395** (1998) 137–143.
9) Xu HE, Stanley TB, Montana VG, Lambert MH, Shearer BG, Cobb JE, Mckee DD, Galardi CM, Plunket KD, Nolte RT, Parks DJ, Moore JT, Kliewer SA, Willson TM, Stimmel JB, Nature **415** (2002) 813–817.
10) Bourguet W, Vivat V, Wurtz JM, Chambon P, Gronemeyer H, Moras D, Mol Cell **5** (2000) 289–298.
11) Yoon HG, Wong J, Mol Endocrinol. **20** (2006) 1048–1060.
12) Willaims SP, Sigler PB, Nature **393** (1998) 392–396.
13) Heery DM, Kalkhoven E, Hoare S, Parker MG, Nature **387** (1997) 733–736.
14) Miyawaki A, Llopis J, Heim R, McCaffery JM, Adams JA, Ikura M, Tsien RY, Nature **388** (1997) 882–887.
15) Sato M, Hida N, Umezawa Y, Proc Natl Acad Sci USA **102** (2005) 14515–14520.
16) Awais M, Sato M, Lee X, Umezawa Y, Angew Chem Int Ed **45** (2006) 2707–2712.
17) Awais M, Sato M, Umezawa Y, Chem Bio Chem **8** (2007) 737–743.
18) St Johnston D, Nat Rev Mol Cell Biol **6** (2005) 363–375.
19) Taanman, J.W, Biochim Biophys Acta **1410** (1999) 103–123.
20) Wang X, McLachlan J, Zamore PD, Hall TM, Cell **110** (2002) 501–512.
21) Shav-Tal Y, *et al*. Science **304** (2004) 1797–1800.
22) Shestakova EA, Singer RH, Condeelis J, Proc Natl Acad Sci USA **98** (2001) 7045–7050.
23) Forrest KM, Gavis ER, Curr Biol **13** (2003) 1159–1168.
24) Huttelmaier S, *et al*. Nature **438** (2005) 512–515.
25) Ozawa T, Natori Y, Sato M, Umezawa Y, Nature Methods **4** (2007) 413–419.
26) Ghosh I, Hamilton AD, Regan L, J Am Chem Soc **122** (2000) 5658–5659.
27) Hu CD, Kerppola TK, Nat. Biotechnol **21** (2003) 539–545.
28) Cheong CG, Hall TM, Proc Natl Acad Sci USA **103** (2006) 13635–13639.
29) Magliery TJ, *et al*. J Am Chem Soc **127** (2005) 146–157.
30) Bota DA, Davies KJ, Nat Cell Biol **4** (2002) 674–680.
31) Chen XJ, Wang X, Kaufman BA, Butow RA, Science **307** (2005) 714–717.
32) Lyamzaev KG, *et al*. Acta Biochim Pol **51** (2004) 553–562.
33) Bota DA, Davies KJ, Mitochondrion **1** (2001) 33–49.
34) Bai Y, Attardi G, EMBO J **17** (1998) 4848–4858.
35) Neupert W, Brunner M, Nat Rev Mol Cell Biol **3** (2002) 555–565.
36) Rehling P, Brandner K, Pfanner N, Nat Rev Mol Cell Biol **5** (2004) 519–530.
37) Truscott KN, Brandner K, Pfanner N, Curr Biol **13** (2003) R326–R337.
38) Allen S, Lu H, Thornton D, Tokatlidis K, J Biol Chem **278** (2003) 38505–38513.
39) Curran SP, Leuenberger D, Oppliger W, Koehler CM, EMBO J **21** (2002) 942–953.
40) Curran SP, Leuenberger D, Leverich EP, Hwang DK, Beverly KN, Koehler CM, J Biol Chem **279** (2004) 43744–43751.
41) Lu H, Allen S, Wardleworth L, Savory P, Tokatlidis K, J Biol Chem **279** (2004) 18952–18958.
42) Lutz T, Neupert W, Herrmann JM, EMBO J **22** (2003) 4400–4408.
43) Zhang J, Campbell RE, Ting AY, Tsien RY, Nat Rev Mol Cell Biol **3** (2002) 906–918.
44) Abad MF, Di Benedetto G, Magalhaes PJ, Filippin L, Pozzan T, J Biol Chem **279** (2004) 11521–11529.
45) Matsuyama S, Llopis J, Deveraux QL, Tsien RY, Reed JC, Nat Cell Biol **2** (2000) 318–325.
46) Llopis J, McCaffery JM, Miyawaki A, Farquhar

MG, Tsien RY, Proc Natl Acad Sci USA **95** :(1998) 6803–6808.
47) Filippin L, Abad MC, Gastaldello S, Magalhaes PJ, Sandona D, Pozzan T, Cell Calcium **37** (2005) 129–136.
48) Hanson GT, Aggeler R, Oglesbee D, Cannon M, Capaldi RA, Tsien RY, Remington SJ, J Biol Chem **279** (2004) 13044–13053.
49) Holliger P, Hudson PJ, Nat Biotechnol **23** (2005) 1126–1136.
50) Reinman M, Jantti J, Alfthan K, Keranen S, Soderlund H, Takkinen K, Yeast **20** (2003) 1071–1084.
51) Biocca S, Cattaneo A, Trends Cell Biol **5** (1995) 248–252.
52) Caron de Fromentel C, Gruel N, Venot C, Debussche L, Conseiller E, Dureuil C, Teillaud JL, Tocque B, Bracco L, Oncogene **18** (1999) 551–557.
53) Du C, Fang M, Li Y, Li L, Wang X, Cell **102** (2000) 33–42.
54) Verhagen AM, Ekert PG, Pakusch M, Silke J, Connolly LM, Reid GE, Moritz RL, Simpson RJ, Vaux DL, Cell **102** (2000) 43–53.
55) Burri L, Strahm Y, Hawkins C J, Gentle IE, Puryer MA, Verhagen A, Callus B, Vaux D, Lithgow T, Mol Biol Cell **16** (2005) 2926–2933.
56) Liu Z, Sun C, Olejniczak ET, Meadows RP, Betz SF, Oost T, Herrmann J, Wu JC, Fesik SW, Nature **408** (2000) 1004–1008.
57) Chai J, Du C, Wu JW, Kyin S, Wang X, Shi Y, Nature **406** (2000) 855–862.
58) Wu G, Chai J, Suber TL, Wu JW, Du C, Wang X, Shi Y, Nature **408** (2000) 1008–1012.
59) Ozawa T, Natori Y, Sako Y, Kuroiwa H, Kuroiwa T, Umezawa Y, ACS Chem Biol **2** (2007) 176–186.
60) Cyr DM, Ungermann C, Neupert W, Methods Enzymol **260** (1995) 241–252.
61) Fuller KM, Arriaga EA, Curr Opin Biotechnol **14** (2003) 35–41.
62) Ozawa T, Sako Y, Sato M, Kitamura T, Umezawa Y, Nat Biotechnol **21** (2003) 287–293.
63) Paulus H, Annu Rev Biochem **69** (2000) 447–496.